

Design and Fabrication of 3-RPS Robot - Rack and Pinion Mechanism

Himanshu V Vairagade
Student, PGDIR
RTMNU's OCE
Nagpur, India
himanshuvairagade1310@gmail.com

Vivek Gurve
Student, PGDIR
RTMNU's OCE
Nagpur, India
vivekgurve.gk@gmail.com

Neema Amish Ukani
HoD, PGDIR
RTMNU's OCE
Nagpur, India
neema.ukani@gmail.com

Sandeep Sonaskar
Asst. Prof., PDGIR
RTMNU's OCE
Nagpur, India
sandeepsonaskar@gmail.com

Saurabh S. Chakole
Asst. Prof., PDGIR
RTMNU's OCE
Nagpur, India
saurabhchakole89@gmail.com

Abstract—Parallel Manipulator is one of the trending research topics in the field of robotics. Recently, the 3-RPS parallel manipulator is widely being used for novel applications. Conventionally, the prismatic actuation is implemented using pneumatic drives. In this paper, a rack and pinion mechanism for prismatic link actuation is proposed. Three different modes of operations and two methods for controls are proposed. To validate the kinematic analysis of this configuration a MATLAB model is developed. To compare the numerical and experimental micro-manipulations two test cases are designed and results are compared.

Index Terms—3-RPS, Parallel Manipulator, Rack and Pinion Mechanism, Forward Kinematics, Sylvester Dialectic Elimination, Passive Joint, Loop Closure Equation, Servo Motor

I. INTRODUCTION

Parallel Manipulators were invented in the late 1980's. The reason to develop such mechanisms was to overcome the issue of poor rigidity and low payload to weight ratio of serial manipulators. For example, a 6-degree of freedom (DOF) parallel manipulator called as Stewart Gough Platform was developed. However, not all 6 degrees are always used for applications. Therefore, mechanisms with a lower degree of freedom were developed. A 3-RPS parallel manipulator is a 3-DOF manipulator invented by Hunt [7]. It can translate in one direction and rotate about other two. Recently, this manipulator has been used for novel applications like the ankle rehabilitation device [3] and biomimetic snake robot as flexible tool for human surgery [2]. However, in all these mechanisms pneumatic cylinders were used to actuate the prismatic link. The use of pneumatic drives introduces issues like noise, lubrication, and lack of precise control. Other alternative for the actuation of the prismatic link is the rack and pinion mechanism. This paper aims to design and fabricate 3-RPS manipulator using the rack and pinion mechanism.



Fig. 1: A 3-RPS Parallel Manipulator

II. LITERATURE SURVEY

After Hunt invented the 3-RPS mechanism most of the research work was carried out in kinematic analysis, dynamic formulations, and control methodologies. In recent years, novel applications using the 3-RPS manipulators were developed. In 2005, Zhu Dachang, Feng Yanping and Fang Yuefan [1] developed a 3-RPS manipulator for packaging and assembly. The analysis of this robot was done using the screw theory. A bio-inspired hyper-redundant 3-RPS manipulator inspired by snakes was designed by Mintenback and Estana [2] in 2010. This manipulator can be used as a flexible tool in human surgery. Nurahmi, Latifah, et al [3] in 2017 developed an Ankle Rehabilitation Device using the 3-RPS. A Vectored Thruster for Autonomous underwater vehicles (AUV's) was developed by Liu and Tao [4] in 2017. The mechanism improved the performance of the AUV's at zero and low forward speed [4]. This mechanism made the AUV

compact and improved the positional accuracy and response time. Zheng and Tao [5] in 2019 developed a novel Three Extensible Rod (TER) mechanism based on a 3-RPS structure. This was developed for the design of space large deployable paraboloid structure with power and communication integration (SSPCI) [5]. The 3-RPS mechanism provided a simple and lightweight structure with high structural stiffness, low inertia, and accurate positioning of the mobile platform.

| Year | Author | Mechanism | Mode of Operations |
|------|--|----------------------------------|--------------------|
| 2010 | Mintenbeck and Estana | Biomimetic Hyper Redundant 3-RPS | Linear Actuators |
| 2017 | Liu, Hu, Xu, Wang, and Du | Vectored Thruster for AUV's | Pneumatic Drives |
| 2019 | Zheng T., Zheng F., Rui, Yan, Niu, and Zhang | Three Extensible Rod Mechanism | Extensible Rods |

TABLE I: Designs of Prismatic Links for 3-RPS Robots

The focus of the above literature survey was on the application based research work of the 3-RPS parallel manipulator. Unlike serial manipulators, there are very few applications for this type of manipulators. Till 2000, there has been intensive research work done in field of kinematics and dynamics of the 3-RPS, Lately, this manipulators are been used for variety of application.

However, in all the applications stated above pneumatic drives are only used for actuation (as shown in Table I). Another alternative for this prismatic link actuation is the rack and pinion mechanism. From the Table II it is evident that rack and pinion mechanism is potential alternative for prismatic actuation. The motivation behind this research is to fabricate a 3-RPS manipulator using rack and pinion mechanism.

| Pneumatic Drives | Rack and Pinion Mechanism |
|-----------------------------------|---|
| Air Leakage | Electricity is relatively cheap than compressed air |
| Loud Noise | Compatible with other smart electronics components |
| Air Choking due to excessive flow | High Precision |

TABLE II: Comparison between different types of actuation of prismatic link

III. PROPOSED WORK

A. Constructive Details

This manipulator consists of two mechanisms: The rack and pinion mechanism and the 3-RPS parallel manipulator.

1) *The 3-RPS Manipulator*: The manipulator consists of a base, an end effector platform, and three limbs of actuator links that are attached to the end effector and base platforms. Using spherical and revolute joint, a link is attached to the base and end-effector platform. The joints on the end-effector and base platforms are on the vertices of an equilateral triangle

with the side length of a and g respectively. The axis of the revolute joints is perpendicular to the line passing through the center of the equilateral triangle of base and the center of the revolute joint. The manipulator has 3 degrees of freedom, rotation about the X-axis and Y-axis, and translation along the Z-axis [6].

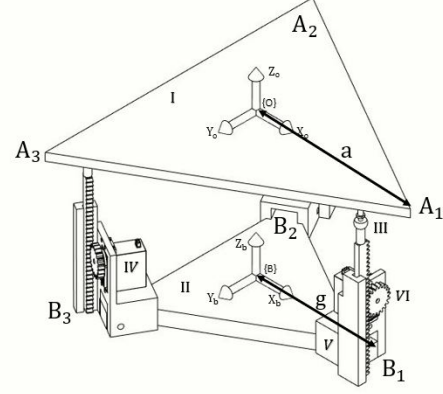


Fig. 2: A 3-RPS Parallel Manipulator

| Number | Component |
|--------|-----------------|
| I | End-Effector |
| II | Base Plate |
| III | Spherical Joint |
| IV | Servo Motor |
| V | Rotary Joint |
| VI | Rack and Pinion |

TABLE III: Components of RPS

The mobility of 3-RPS parallel manipulator can be determined using the Kutzbach-Grübler formula:

$$F = \lambda(n - j - 1) + \sum_{i=1}^j f_i \quad (1)$$

Here, λ is equal 6, since 3-RPS is a spatial manipulator, n is the number of links, j is the number of joints connecting only two links, f_i is the degrees of freedom of the i^{th} joint. In 3-RPS manipulator, n is equal to 8, j is 9 and $\sum_{i=1}^j f_i$ is 15. Therefore, the mobility is 3.

2) *Rack and Pinion Mechanism*: A rack and pinion mechanism is a linear actuator. It is used to convert rotary motion into linear motion. It consists of a pinion gear that is connected to the motor. A rack that slides on a pinion providing translation. We need to derive the relation between the rotation of pinion and translation of rack.

Considering D as the pitch diameter of the pinion, the circumference will be:

$$C = \pi D \quad (2)$$

From this using the pitch diameter of the pinion gear we can obtain the circumference. The circumference when divided by 360deg will yield the actuation per degree of the servo motor.

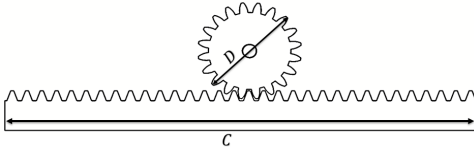


Fig. 3: Rack and Pinion Mechanism

B. Kinematics

Kinematics is the study of robot's geometry and position without considering the forces and moments acting on it. It is the fundamental analysis which explains the working of a mechanism. This consists of two types - Forward and Inverse. The parallel manipulator usually consists of passive joints and multi-DOF joints which makes the kinematic analysis different from that of serial manipulators.

1) *Forward Kinematics*: This is also called Direct Kinematics. The goal is to obtain the end-effector's position and orientation given the joint variables as the inputs. Unlike, serial manipulators the forward kinematics of parallel mechanism is complex due to the presence of closed-loop and passive joints.

To perform the forward kinematics of the 3-RPS parallel manipulator first we need to express the passive joints in terms of the active joints. Furthermore, we need to derive the position of the centroid of the end-effector platform. Consider $(\theta_1, \theta_2, \theta_3)$ as the passive joints and (l_1, l_2, l_3) are the active prismatic joints for the derivation of the kinematics of manipulator. Here, ρ is the ratio of a and g the length from center to vertices for the end effector and base platform.

2) *Loop Closure Equation*: In the 3-RPS mechanism, there are three passive joints and three active joints. To calculate the position 3 additional equations will be needed. These additional equations are constraint or loop closure equations. Loop closure simply means going around a closed-loop of parallel manipulator. In the 3-RPS, from the centroid of the base-platform via the passive rotary joint and the limb of manipulator we reach the spherical joints. As there are three spherical joints we can obtain three paths, one for every joint. Using the fact that, the length of side of the end-effector is constant $\sqrt{3}a$ (side of an equilateral triangle) we can get 3 equations in terms of active and passive joints. Now, we can use these three loop closure equations to obtain the passive variables in terms of active variables.

$$\begin{aligned} \text{loop1} = & -3l_1 \cos(\theta_1) - 3l_2 \cos(\theta_2) + l_1^2 - 3\rho^2 + 3 \\ & l_1 l_2 \cos(\theta_1) \cos(\theta_2) + l_2^2 - 2l_1 l_2 \end{aligned} \quad (3)$$

$$\begin{aligned} \text{loop2} = & -3l_2 \cos(\theta_2) - 3l_3 \cos(\theta_3) + l_2^2 - 3\rho^2 + 3 \\ & l_2 l_3 \cos(\theta_2) \cos(\theta_3) + l_3^2 - 2l_2 l_3 \end{aligned} \quad (4)$$

$$\begin{aligned} \text{loop3} = & -3l_1 \cos(\theta_1) - 3l_3 \cos(\theta_3) + l_1^2 - 3\rho^2 + 3 \\ & l_1 l_3 \cos(\theta_1) \cos(\theta_3) + l_3^2 - 2l_1 l_3 \end{aligned} \quad (5)$$

3) *Sylvester Dialectic Elimination*: The loop closure equations are polynomial expression with an order of 2. Solving this simultaneously is complex. Therefore, an elimination method called Sylvester Dialectic Elimination is applied. This method basically converts the equations into polynomial form and creates a uni-variate polynomial expression. This polynomial is of the order of 16. Out of the 16 roots 8 are imaginary and can be neglected. Based on the geometrical constraints of the 3-RPS, positive roots are selected. Using these positive real roots, the other two passive variables are calculated.

In order to obtain the position of the end effector's centroid, the position of the spherical joints are calculated. Lee and Shah [14] proposed the formulas for the position of the spherical joints in terms of the active and passive joint variables as:

$$\begin{aligned} X_{s1} &= 1 - l_1 \cos(\theta_1) \\ Y_{s1} &= 0 \\ Z_{s1} &= l_1 \sin(\theta_1) \end{aligned} \quad (6)$$

$$\begin{aligned} X_{s2} &= -0.5(1 - l_2 \cos(\theta_2)) \\ Y_{s2} &= \frac{\sqrt{3}}{2}(1 - l_2 \cos(\theta_2)) \\ Z_{s2} &= l_2 \sin(\theta_2) \end{aligned} \quad (7)$$

$$\begin{aligned} X_{s3} &= -0.5(1 - l_3 \cos(\theta_3)) \\ Y_{s3} &= \frac{-\sqrt{3}}{2}(1 - l_3 \cos(\theta_3)) \\ Z_{s3} &= l_3 \sin(\theta_3) \end{aligned} \quad (8)$$

These spherical joints are nothing but the vertices of the equilateral triangle. The centroid (X_c, Y_c, Z_c) can be obtained as:

$$\begin{aligned} X_c &= \frac{1}{3}(X_{s1} + X_{s2} + X_{s3}) \\ Y_c &= \frac{1}{3}(Y_{s1} + Y_{s2} + Y_{s3}) \\ Z_c &= \frac{1}{3}(Z_{s1} + Z_{s2} + Z_{s3}) \end{aligned} \quad (9)$$

The orientation of the end-effector can be expressed in terms of Z-Y-Z Euler angles (α, β, γ) . These angles can be calculated with the position of the centroid as:

$$\begin{aligned} \alpha + \gamma &= \pi \\ X_c &= -\frac{1}{2}\rho \cos(2\alpha)(1 - \cos(\beta)) \\ Y_c &= \frac{1}{2}\rho \sin(2\alpha)(1 - \cos(\beta)) \end{aligned} \quad (10)$$

C. Experimental Setup

For this manipulator, some components were procured from the market and others were fabricated. The base and end-effector triangular plates were fabricated from sheets of acrylic. The rack, pinion gear, and spherical bearing were procured from the market and the clamp structure for the rack and pinion was manufactured using wood.

The Table IV lists the major dimensions of the manipulator.

| Dimension | Value |
|------------------------|--------|
| Base Plate(g) | 110 mm |
| End Effector Plate(a) | 140 mm |
| Rack Length | 145 mm |
| Pinion Diameter | 50 mm |
| Number of teeth Pinion | 50 |
| Number of teeth Rack | 39 |

TABLE IV: Dimensions of 3-RPS

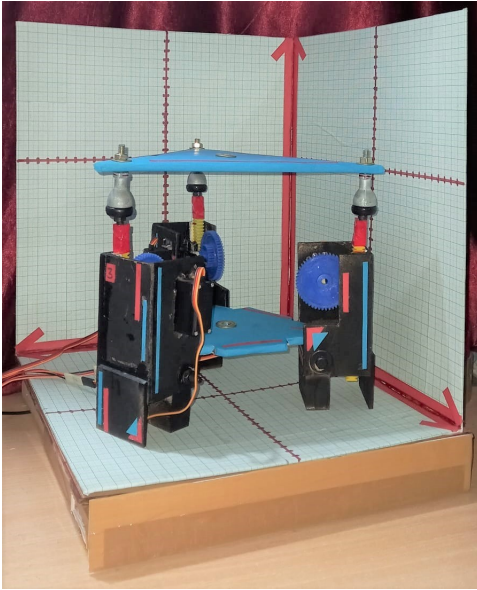


Fig. 4: Complete Assembly

The electronics components used in this project are:

- ATmega328P Arduino Uno
- PS2 Joystick Module
- HC-05 Bluetooth Module
- PL2303 USB to TTL (used as power source for the servo motor)

To control the servo motor of the prismatic link, two types of control methods are proposed. First method is to control using the joystick module and in the other method, the motors are controlled using a mobile application. In the joystick control method, a home position is defined, and the manipulator goes back to this position after the joystick is released. However, in control via mobile application, the manipulator can be held static at any given position. However, the response time of mobile application is high compared to the joystick control.

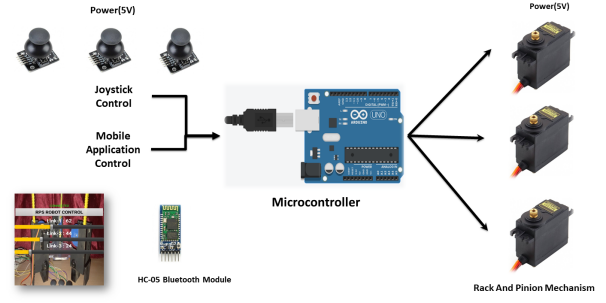
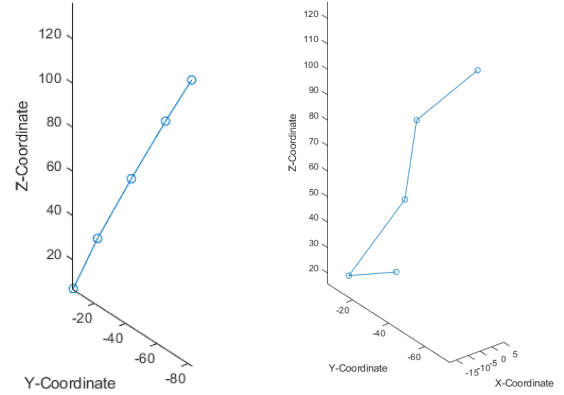


Fig. 5: Control Architecture



(a) Test Case - 1

(b) Test Case - 2

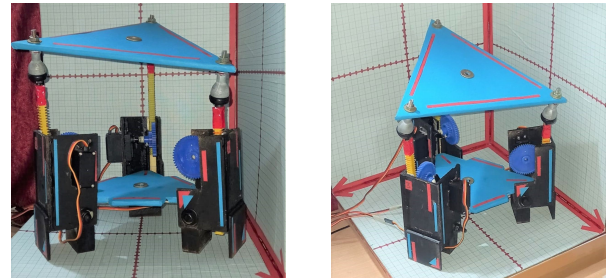
Fig. 6: Trajectory of Test Cases



(a) Front

(b) Isometric

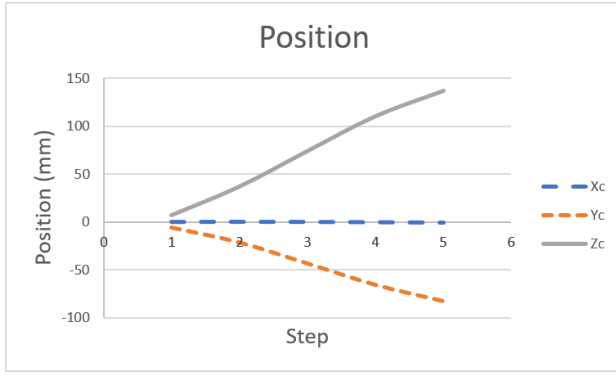
Fig. 7: Test Case-1



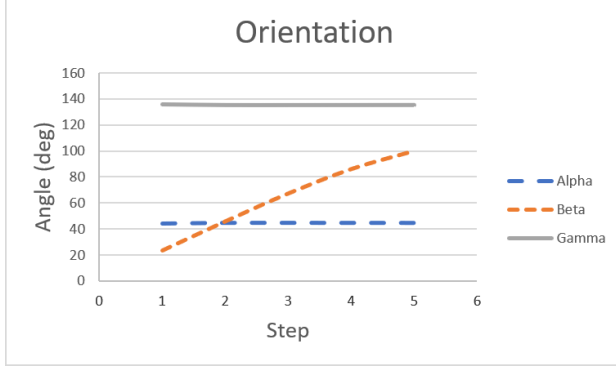
(a) Front

(b) Isometric

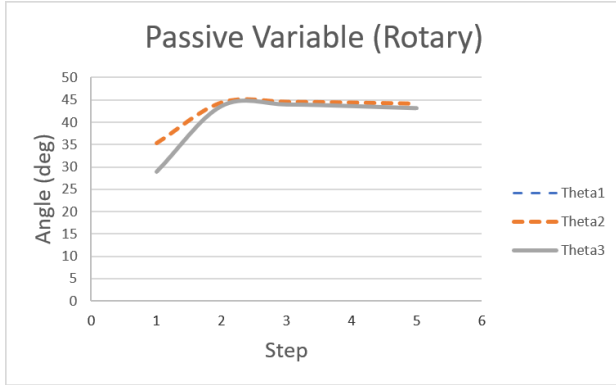
Fig. 8: Test Case-2



(a) Position Plot

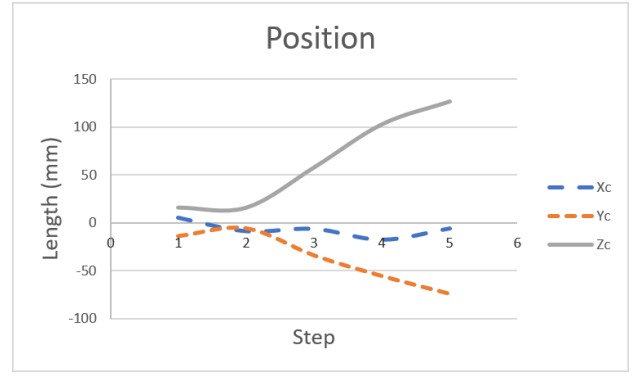


(b) Orientation Plot

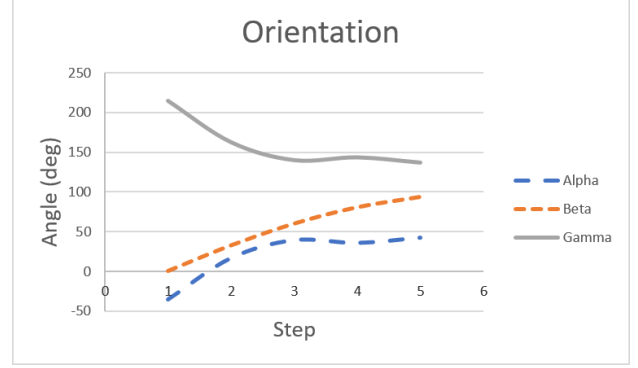


(c) Passive Joints Plot

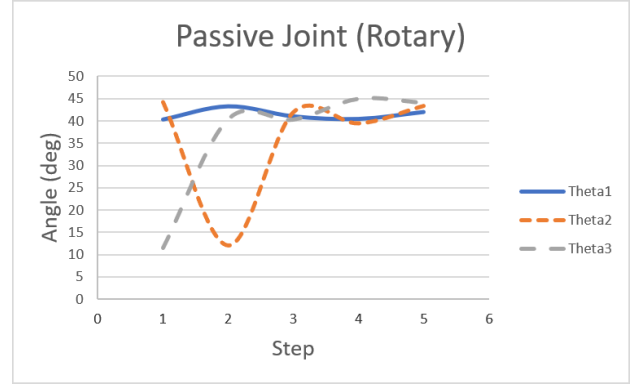
Fig. 9: Plots for Test Case-1



(a) Position Plot



(b) Orientation Plot



(c) Passive Joints Plot

Fig. 10: Plots for Test Case-2

D. Numerical and Experimental Simulation

In order to validate the kinematics, a numerical model for the forward kinematics was developed in MATLAB. The inputs are the servo angles (s_1, s_2, s_3) for the three servos respectively. The model converts these angles to respective lengths of pinion using the actuation length per degree of the rack and pinion mechanism. Then, the passive variables are calculated using the loop closure equations and Sylvester dialectic elimination. Both the active and passive joint variables are given as inputs to the forward kinematics model and the position and orientation of the end effector centroid are calculated.

A set of test cases describing the variation of the servo

angles is designed. The trajectories specify servo angles input at discrete steps. Each of the cases consists of 5 such steps. The characteristics of which are:

- **Test Case-1** : To test the ability of translation about the Z-axis this case is designed. In this, the servo angles at each step are equal.
- **Test Case-2** : To realise the combined translation and rotation of the end-effector this case is designed. A non-uniform trajectory of servo angles is designed.

Figure 6 shows the plot of trajectory for both cases. Table VIII describes the numerical and experimental results of both the test cases.

TABLE V: Test Case -1 Numerical Simulations

| Servo Angles | | | | Joint Variables | | | | | | End-Effector Pose | | | | | |
|--------------|-------|-------|-------|-----------------|---------|---------|------------|------------|------------|-------------------|---------|---------|----------|---------|----------|
| Step | S_1 | S_2 | S_3 | l_1 | l_2 | l_3 | θ_1 | θ_2 | θ_3 | X_c | Y_c | Z_c | α | β | γ |
| 1 | 10 | 10 | 10 | 13.235 | 13.235 | 13.235 | 28.950 | 35.304 | 28.950 | -0.130 | -5.884 | 6.821 | 44.367 | 23.663 | 135.633 |
| 2 | 40 | 40 | 40 | 52.940 | 52.940 | 52.940 | 43.581 | 44.372 | 43.581 | -0.085 | -21.417 | 36.671 | 44.887 | 46.050 | 135.113 |
| 3 | 80 | 80 | 80 | 105.880 | 105.880 | 105.880 | 43.912 | 44.528 | 43.912 | -0.132 | -43.232 | 73.705 | 44.912 | 67.518 | 135.088 |
| 4 | 120 | 120 | 120 | 158.820 | 158.820 | 158.820 | 43.564 | 44.356 | 43.564 | -0.254 | -65.425 | 109.980 | 44.889 | 86.253 | 135.111 |
| 5 | 150 | 150 | 150 | 198.525 | 198.525 | 198.525 | 43.096 | 44.118 | 43.096 | -0.407 | -82.413 | 136.492 | 44.859 | 100.215 | 135.141 |

TABLE VI: Test Case -2 Numerical Simulations

| Servo Angles | | | | Joint Variables | | | | | | End-Effector Pose | | | | | |
|--------------|-------|-------|-------|-----------------|---------|---------|------------|------------|------------|-------------------|---------|---------|----------|---------|----------|
| Step | S_1 | S_2 | S_3 | l_1 | l_2 | l_3 | θ_1 | θ_2 | θ_3 | X_c | Y_c | Z_c | α | β | γ |
| 1 | 10 | 40 | 10 | 13.235 | 52.940 | 13.235 | 40.377 | 44.274 | 11.475 | 5.119 | -14.109 | 16.055 | -35.030 | 0.000 | 215.030 |
| 2 | 40 | 10 | 10 | 52.940 | 13.235 | 13.235 | 43.278 | 11.982 | 40.319 | -9.008 | -6.073 | 15.868 | 16.994 | 32.349 | 163.006 |
| 3 | 80 | 40 | 80 | 105.880 | 52.940 | 105.880 | 41.068 | 41.983 | 40.237 | -6.579 | -34.115 | 57.788 | 39.543 | 59.758 | 140.457 |
| 4 | 150 | 80 | 120 | 198.525 | 105.880 | 158.820 | 40.494 | 39.490 | 44.900 | -17.956 | -55.486 | 102.785 | 36.034 | 80.394 | 143.966 |
| 5 | 150 | 120 | 150 | 198.525 | 158.820 | 198.525 | 42.025 | 43.417 | 43.999 | -6.129 | -73.951 | 126.655 | 42.631 | 93.443 | 137.369 |

TABLE VII: Test Case -1 Experimental Observations

| Input | | | | End-Effector Pose | | | | | |
|--------------|-------|-------|-------|-------------------|-------|-------|-------------|---------|----------|
| Servo Angles | | | | Position | | | Orientation | | |
| Step | S_1 | S_2 | S_3 | X_c | Y_c | Z_c | α | β | γ |
| 1 | 10 | 10 | 10 | -0.16 | -7 | 5.9 | 44.345 | 25.845 | 135.65 |
| 2 | 40 | 40 | 40 | -0.06 | -19 | 32 | 44.345 | 25.845 | 135.65 |
| 3 | 80 | 80 | 80 | -0.16 | -38 | 64 | 44.879 | 62.797 | 135.12 |
| 4 | 120 | 120 | 120 | -0.2 | -75 | 97 | 44.924 | 94.096 | 135.08 |
| 5 | 150 | 150 | 150 | -0.5 | -71 | 118 | 44.798 | 90.82 | 135.2 |

TABLE VIII: Test Case -2 Experimental Observations

| Input | | | | End-Effector Pose | | | | | |
|--------------|-------|-------|-------|-------------------|-------|-------|-------------|---------|----------|
| Servo Angles | | | | Position | | | Orientation | | |
| Step | S_1 | S_2 | S_3 | X_c | Y_c | Z_c | α | β | γ |
| 1 | 10 | 40 | 10 | 4 | -16 | 15 | -37.982 | 0 | 217.98 |
| 2 | 40 | 10 | 10 | -8 | -5 | 18 | 16.003 | 30.091 | 164 |
| 3 | 80 | 40 | 80 | -5 | -30 | 55 | 40.269 | 55.562 | 139.73 |
| 4 | 150 | 80 | 120 | -15 | -50 | 95 | 36.65 | 75.27 | 143.35 |
| 5 | 150 | 120 | 150 | -5 | -65 | 105 | 42.801 | 86.062 | 137.2 |

IV. RESULTS AND DISCUSSION

A. General Inferences

Based on the numerical simulations and experiments the error in the position and orientation of the 3-RPS manipulator is tabulated below in Table IX. From this data,

the position, orientation and the passive variable plots are generated. The average absolute error in measurements of X_c, Y_c, Z_c is 20.9%, 13.5%, 11.4% respectively. The overall error in the orientation measurement is 15.3%. The average absolute error in the orientation measurement α, β, γ is 0.05%,

| Step | Test Case - 1 | | | | | | Test Case - 2 | | | | | |
|------|---------------|------------|------------|---------------|--------------|---------------|---------------|------------|------------|---------------|--------------|---------------|
| No | Err% X_c | Err% Y_c | Err% Z_c | Err% α | Err% β | Err% γ | Err% X_c | Err% Y_c | Err% Z_c | Err% α | Err% β | Err% γ |
| 1 | 23.08 | 18.97 | 13.50 | 0.05 | 9.22 | 0.01 | 21.86 | 13.40 | 6.57 | 8.43 | 0.00 | 1.37 |
| 2 | 29.41 | 11.29 | 12.74 | 0.05 | 6.12 | 0.02 | 11.19 | 17.67 | 13.44 | 5.83 | 6.98 | 0.61 |
| 3 | 21.21 | 12.10 | 13.17 | 0.07 | 6.99 | 0.02 | 24.00 | 12.06 | 4.83 | 1.84 | 7.02 | 0.52 |
| 4 | 21.26 | 14.64 | 11.80 | 0.08 | 9.09 | 0.02 | 16.46 | 9.89 | 7.57 | 1.71 | 6.37 | 0.43 |
| 5 | 22.85 | 13.85 | 13.55 | 0.14 | 9.37 | 0.04 | 18.42 | 12.10 | 17.10 | 0.40 | 7.90 | 0.12 |

TABLE IX: Error Table for Test Cases

6.90% and 0.31% respectively. The overall error in orientation measurement is 2.42%. The main source of error is a human observational error. However, the error is below the limit of approximately 15% therefore the model is validated.

B. Inferences of Test Case-1

In test case-1, only the translation in Z axis occurs, this is validated by the graphs of Figure 9. The Z_c coordinate is changing linearly with steps and also the orientation is constant for the entire trajectory. Due to the friction less spherical joint, there is a deflection observed in y-coordinate and β . It is interesting to note that the change in passive joint variables obtained from the Sylvester Dialectic elimination method is minimal. This can be attributed to the lack of rotation in this test case.

C. Inferences of Test Case-2

As the test case-2 consists of non-uniform actuation which leads to both translation and rotation of the end-effector. This characteristic is evident from the position and orientation graphs of Figure 10. Unlike the test case-1, here there are significant and non-uniform changes in the values of all passive joints. We can conclude that the passive joint value depends upon the type of trajectory of the manipulator.

V. CONCLUSION

In this paper, the 3-RPS manipulator is designed using the rack and pinion mechanism. The manipulator can achieve a maximum height of 130 mm with rotations about the X and Y axes. A MATLAB model of forward kinematics is developed with two unique test cases designed for validation. The average error in position and orientation is 15.3% and 2.42% respectively. It can be concluded that the type of trajectory will influence the changes in passive joints. The work presented here validated the rack and pinion mechanism. Furthermore, a design of rack and pinion mechanism can be carried out for a specific application. However, the rack and pinion can get unstable for long height of rack. This 3-RPS model can be developed depending upon the application and can serve as a good alternative to the conventional linear actuators using pneumatic drives.

REFERENCES

[1] Dachang, Zhu, Feng Yanping, and Fang Yuefeng. "A novel parallel manipulator design for packaging and assembly." 2005 6th International Conference on Electronic Packaging Technology. IEEE, 2005.

[2] J. Mintenbeck and R. Estaña, "Design, modelling and control of a hyper-redundant 3-RPS parallel mechanism," 2010 IEEE International Conference on Robotics and Biomimetics, Tianjin, China, 2010, pp. 591-596, doi: 10.1109/ROBIO.2010.5723392.

[3] Nurahmi, Latifah, et al. "Dimension synthesis of 3-RPS parallel manipulator with intersecting R-axes for ankle rehabilitation device." 2017 18th International Conference on Advanced Robotics (ICAR). IEEE, 2017.

[4] Liu, Tao, et al. "A novel vectored thruster based on 3-RPS parallel manipulator for autonomous underwater vehicles." Mechanism and Machine Theory 133 (2019): 646-672.

[5] Zheng, Tao, et al. "Analysis of a three-extensible-rod tracker based on 3-RPS parallel manipulator for space large deployable paraboloid structure with power and communication integration." Acta Astronautica 169 (2020): 1-22.

[6] D. Zhao, W. Hailong, Z. Hongyan, and N. Tao, "Explicit solution for inverse kinematics of 3-rps parallel link manipulator," in 2010 International Conference on Computer, Mechatronics, Control and Electronic Engineering, vol. 2. IEEE, 2010, pp. 425-429.

[7] K.H. Hunt, Structural kinematics of in-parallel actuated robot arms, ASME Journal of Mechanisms, Transmissions, and Automation in Design 105 (1983) 705-712.

[8] Lee, Kok-Meng and Shah, Dharman. (1988). Kinematic analysis of a three-degrees-of-freedom in-parallel actuated manipulator. Robotics and Automation, IEEE Journal of. 4. 354 - 360. 10.1109/56.796.

[9] Parasuraman, S. and P. J. Liang. "Development of RPS Parallel Manipulators." 2010 Second International Conference on Computer and Network Technology (2010): 600-605.

[10] Mohan Rao, Nalluri and Rao, K.. (2009). Dimensional synthesis of a spatial 3-RPS parallel manipulator for a prescribed range of motion of spherical joints. Mechanism and Machine Theory. 44. 477-486. 10.1016/j.mechmachtheory.2008.03.001.

[11] H. Z. Arabshahi and A. B. Novinzadeh, "Impedance control of the 3RPS parallel manipulator," 2014 Second RSI/ISM International Conference on Robotics and Mechatronics (ICRoM), Tehran, Iran, 2014, pp. 486-492, doi: 10.1109/ICRoM.2014.6990949.

[12] Nurahmi, Latifah, and Mochamad Solichin. "Motion type of 3-RPS parallel manipulator for ankle rehabilitation device." 2017 international conference on advanced mechatronics, intelligent manufacture, and industrial automation (ICAMIMIA). IEEE, 2017.

[13] Schadlbauer, Josef et al. "A Complete Kinematic Analysis of the 3-RPS Parallel Manipulator." (2011).

[14] Lee, Kok-Meng and Shah, Dharman. (1988). Kinematic analysis of a three-degrees-of-freedom in-parallel actuated manipulator. Robotics and Automation, IEEE Journal of. 4. 354 - 360. 10.1109/56.796.

[15] Mohan Rao, Nalluri and Rao, K.. (2009). Dimensional synthesis of a spatial 3-RPS parallel manipulator for a prescribed range of motion of spherical joints. Mechanism and Machine Theory. 44. 477-486. 10.1016/j.mechmachtheory.2008.03.001.

[16] YIN, Bao-Lin and YAN, Bing-Bing and SHUAI, Jun-Feng and REN, Wen-Bo. (2014). Solution for Direct Kinematics of 3-PRS Parallel Manipulator Using Sylvester Dialectic Elimination Method. 10.2991/icmce-14.2014.27.

[17] Rad, Ciprian-Radu and Stan, Sergiu-Dan and Balan, Radu and Lapusan, Ciprian. (2010). Forward kinematics and workspace analysis of a 3-RPS medical parallel robot. 2010 IEEE International Conference on Automation, Quality and Testing, Robotics, AQTR 2010 - Proceedings. 1. 1 - 6. 10.1109/AQTR.2010.5520867.

[18] Yin, B., Yan, B., Shuai, J., and Wen-bo, R. (2014). Solution for Direct Kinematics of 3-PRS Parallel Manipulator Using Sylvester Dialectic Elimination Method.